International Immunopharmacology 73 (2019) 333–342

Contents lists available at ScienceDirect

International Immunopharmacology

journal homepage: www.elsevier.com/locate/intimp

Growth arrest-specific protein 6 (Gas6) attenuates inflammatory injury and apoptosis in iodine-induced NOD.H-2^{h4} mice

Xuren Sun[a], Haixia Guan[b,*,1], Shiqiao Peng[b], Yu Zhao[b], Le Zhang[c], Xinyi Wang[d], Chenyan Li[b,*,1], Zhongyan Shan[b], Weiping Teng[b]

[a] Department of Gastroenterology, The First Affiliated Hospital of China Medical University, Shenyang, Liaoning 110001, PR China
[b] Department of Endocrinology and Metabolism, Institute of Endocrinology, Liaoning Provincial Key Laboratory of Endocrine Diseases, The First Affiliated Hospital of China Medical University, Shenyang, Liaoning 110001, PR China
[c] The Second Department of Endocrinology, Sheng Jing Affiliated Hospital of China Medical University, Shenyang, Liaoning 110001, PR China
[d] Department of Laboratory Medicine, The First Affiliated Hospital of China Medical University, China Medical University, Shenyang, Liaoning 110001, PR China

ARTICLE INFO

Keywords:
Growth arrest-specific protein 6
Apoptosis
TAM receptors
NOD.H-2^{h4} mice

ABSTRACT

Purpose: Growth arrest-specific protein 6 (Gas6) is a vitamin K-dependent protein that plays an important role in the pathogenesis of autoimmune diseases. The purpose of this study was to explore the expression of Gas6 and its effects on autoimmune thyroiditis (AIT).

Method: A total of 24 male NOD.H-2^{h4} mice were randomly assigned to three groups: (1) a control group supplied with regular water; (2) a sodium iodide (NaI) group supplied with 0.005% sodium iodide water; and (3) a group treated with recombinant mouse Gas6 (rmGas6) after iodine supplementation (NaI + Gas6 group). The severity of lymphocytic infiltration in the thyroid was measured through histopathology. Serum levels of tumor necrosis factor α (TNF-α), interleukin (IL) 6 and IL-1β, as well as anti-thyroglobulin antibody (TgAb) titers were measured using an enzyme-linked immunosorbent assay. In addition, the expression of Gas6, Caspase 3, TAM receptors (Axl and MerTK), nuclear factor κB (NF-κB) and I-kappa-B α (IκB-α) were measured by Western blotting. Finally, the proportions of T cells were determined in the splenocytes of NOD.H-2^{h4} mice by flow cytometry.

Results: The mRNA and protein expression of Gas6 was significantly lower in the NaI group compared to the control group. Serum levels of TgAb, TNF-α, IL-6 and IL-1β were also significantly higher in the NaI group but were dramatically reduced after rmGas6 injection. The prevalence of thyroiditis and the infiltration of lymphocytes were significantly lower in the NaI + Gas6 group compared to the NaI group. The protein expression of cleaved-Caspase 3, phosphorylation of MerTK, and NF-κB and IκB-α in the thyroid gland were significantly reduced after rmGas6 administration. The proportion of Th1, Th2 and Th17 cells in splenocytes were also significantly reduced after rmGas6 treatment, whereas there was a dramatic increase in the proportion of Treg cells.

Conclusion: Gas6 exerts an anti-inflammatory effect in a mouse model of AIT and may therefore be a potential therapeutic target.

1. Introduction

Autoimmune thyroiditis (AIT) is an organ-specific autoimmune disease characterized by the infiltration of lymphocytes into the thyroid gland [1]. AIT, also known as Hashimoto's thyroiditis, is the primary reason for hypothyroidism [2], which develops as a consequence of a combination of environmental, genetic and immunological factors. Among all environmental factors, an excess of iodine is considered to be the most important in triggering and promoting the development of AIT [1]. However, the exact mechanism underlying iodine-induced AIT remains to be elucidated. Under specific conditions, after modulation by a co-stimulatory molecule, naive CD4$^+$ T lymphocytes can be activated to form different subsets of T lymphocytes, including Th1, Th2 and Th17 cells, and regulatory T cells (Tregs), which have different biological functions. CD4$^+$ T lymphocytes from NOD.H-2^{h4} mice are depleted by injection with an anti-CD4 monoclonal antibody. This

* Corresponding authors at: Department of Endocrinology and Metabolism, Institute of Endocrinology, Liaoning Provincial Key Laboratory of Endocrine Diseases, The First Affiliated Hospital of China Medical University, China Medical University, Shenyang, Liaoning 110001, PR China.
E-mail addresses: hxguan@vip.126.com (H. Guan), chenyan830424@126.com (C. Li).
[1] Chenyan Li and Haixia Guan contributed equally in this work.

https://doi.org/10.1016/j.intimp.2019.04.038
Received 1 August 2018; Received in revised form 15 March 2019; Accepted 18 April 2019
Available online 23 May 2019

treatment significantly decreases the severity of spontaneous AIT (SAT), thus indicating that $CD4^+$ T lymphocytes play an important role in the development of SAT. NOD.H-2^{h4} mice have been derived by hybridizing NOD mice and B10.A (4 R) mice and then backcrossing offspring of the B10.A (4 R) mice expressing the MHC haplotype to NOD mice. MHC haplotype (H-2K) mice are genetically susceptible to autoimmune thyroid diseases. This mouse model displays SAT with TgAbs, and intrathyroid lymphocyte infiltration persists throughout the lifetime. Furthermore, this inflammation is accelerated when the mice are given excess iodine through their drinking water, thus making this model an ideal AIT experimental animal model [3]. The apoptosis of thyroid follicular cells and the infiltration of lymphocytes play crucial roles in the self-breakdown process of AIT. Apoptosis regulates multiple functions in biology, such as the clearance of abnormal cells during development, homeostasis, and the immune response and defense [4,5]. The destruction of thyroid follicular cells *via* apoptosis has been demonstrated to be an important cause of AIT [6]. Apoptotic follicular cells in the thyroid can be identified by macrophages *via* a series of surface receptors. Among these, the TAM (Tyro3, Axl and MerTK) family plays a crucial role in the removal of apoptotic cells by immune cells such as macrophages and dendritic cells [7].

TAM receptors, including Tyro3, Axl and MerTK, are a tyrosine kinase subfamily that plays a crucial role in regulating the innate immune response to acute inflammatory diseases [8]. In the 1990s, Gas6 and Protein S (ProS) were identified as the ligands for TAM receptors [9]. Gas6 has also been reported to activate all TAMs, despite their different binding affinities (Axl > Tyro3 > > > MerTK) [10], whereas ProS activates Tyro3 and MerTK [11,12]. TAM signaling is characterized by the periodic clearance of apoptotic cells from immune cells such as macrophages and dendritic cells in vertebrates, thus suggesting that TAM receptors and their ligands contribute to the reproductive and immune systems [13].

Members of the TAM family of receptors are expressed mainly in immune cells and serve as immune regulators through the phagocytosis of apoptotic cells and the production of signaling suppressors and pro-inflammatory cytokines [14]. MerTK and Axl expressed by macrophages are essential in the clearance of apoptotic fragments and depend upon Gas6 and the regulation of the immune system [15]. Gas6 binds phosphatidylcholine and stimulates phagocytosis and thus the clearance of apoptotic cells *via* the Gla domain.

Gas6 is a vitamin-K dependent protein with high structural homology to the other TAM ligands, such as protein S. Furthermore, Gas6 and ProS share an identical modular structure and 40% sequence similarity. Although Gas6 and ProS are similar, there are still many differences between these two ligands in terms of their biological effects: Gas6 predominantly participates in cell protection and tissue reconstruction [16]. Gas6 acts not only as a protective target in many types of cells but also as a regulator that mediates the production of cytokines [17]. In addition, a previous *in vitro* study has shown that Gas6 decreases production of lipopolysaccharide-induced tumor necrosis factor α (TNF-α), and interleukin (IL) 1β *via* its receptor MerTK, but not *via* Axl or Tyro3 [18]. The inhibition of Gas6 by toll-like receptor stimulation, and the lack of MerTK, results in the upregulation of inflammation [19,20]. Gas6 is present at high levels in inflammatory diseases, but the expression of Gas6 markedly decreases after binding with its receptor, Axl [21]. In this process, Axl shedding occurs, and Gas6 is consequently deactivated. Therefore, we hypothesized that Gas6 might play a protective role by binding its receptor. In a hepatic reperfusion injury model, Gas6 has been found to protect against systematic injury and promote the survival of hepatocytes [22]. Moreover, Gas6 also acts on MerTK and Axl, thus suggesting that Gas6 may be downregulated through the NF-κB pathway and consequently inhibits the inflammatory response [19,23].

The purpose of this study was to elucidate the role of Gas6 in AIT and the mechanisms involved. We used the NOD.H-2^{h4}-mouse model of AIT, triggered by iodine supplementation, to investigate the role of administration of recombinant mouse Gas6 (rmGas6) after thyrocyte damage and systematic inflammation in AIT. We also evaluated the effect of rmGas6 on apoptosis and activation of the NF-κB signaling pathway *in vivo*.

2. Materials and methods

2.1. Mice

NOD.H-2^{h4} mice were purchased from the Jackson Laboratory (Bar Harbor, ME, USA). Animals were fed and raised in the animal facility of China Medical University under specific pathogen controlled conditions and 12 h light/dark cycles, with regular disinfection of cages. Animal care and experimental procedures were applied according to guidelines approved by the Animal Ethics Committee of China Medical University. The NOD.H-2^{h4} mice were raised and housed in the animal facility until 4 weeks of age. Twenty-four male mice were then randomly allocated to three groups (n = 8 per group). Mice in the control group were treated with sterile water. Mice in the sodium iodide (NaI) group were given 0.005% NaI in their drinking water for 8 weeks. Mice in the NaI + Gas6 group received rmGas6 (1 μg/dose; R&D, Minneapolis, MN, USA) by intravenous injection into the tail vein. The vehicle for rmGas6 was normal saline. We treated mice every other day with a total of seven doses of rmGas6. The precise dosage of Gas6 administration was based on that from a previous report by Shibata et al. [24]. The left thyroid lobes of animals in the three groups were removed surgically under anesthesia, washed with cold chlorate water and blotted on filter paper. The thyroid lobes from each group were then frozen at −80 °C until further analysis.

2.2. Assessment of autoimmune thyroiditis

The left thyroid lobe from each NOD.H-2^{h4} mouse, at each experimental time point, was perfused with 4% paraformaldehyde for over 24 h, embedded in paraffin and then sliced into 5-μm sections. Next, sections were stained with hematoxylin and eosin (HE). Changes in thyroid tissue histology were investigated under a light microscope (BX51/BX52, Olympus, Japan). The degree of lymphocyte infiltration was classified as previously described [25]. In brief, HE-stained thyroid sections were scored with the following scale, in accordance with the area occupied by lymphocyte infiltration: 0 = normal; 1+ = 1–10%; 2+ = 10–30%; 3+ = 30–50%; and 4+ > 50%. These histological grades are shown as the means for at least three discontinuous thyroid sections.

2.3. Quantitative real-time PCR analysis

RNA was extracted from thyroid tissues with TRIzol (Invitrogen; Thermo Fisher Scientific Inc., Waltham, MA, USA). First-strand cDNA was then synthesized from total RNA with a reverse transcription kit (TaKaRa Biotechnology Co., Ltd., Dalian, China); glyceraldehyde 3-phosphate dehydrogenase (GAPDH) was used as a control (R&D Systems). The primer sequences used to amplify Gas6 and GAPDH were designed with the ABI PRISM system (Applied Biosystems) and BLAST software from the National Centre for Biotechnology Information (NCBI). The reaction volumes were 20 μl, and gene expression was determined with SYBR Premix II (TaKaRa Biotechnology Co., Ltd.). Reactions were initiated by a 2 min pre-incubation at 95 °C followed by 40 three-step cycles of amplification. PCR was carried out for 40 cycles according to the following procedure: 95 °C for 30 s, annealing for 30 s, and 60 °C for 34 s. Each sample was analyzed in duplicate. Normalized Gas6 mRNA expression was determined through the comparative Ct method, with GAPDH as a reference. The relative mRNA expression levels of the target genes were calculated with the $2^{-\Delta Ct}$ method after normalization to GAPDH. The mRNA sequences used for PCR were as follows: Gas6, 5′-CGAGTCTTCTCACACTGCTGTT-3′ (forward); 5′-GCA

CTCTTGATATCGTGGATAGAAATAC-3′ (reverse); GAPDH, 5′-TGGTGA AGGTCGGTGTGAAC-3′ (forward); 5′-CCATGTAGTTGAGGTCAATGA AGG-3′ (reverse).

2.4. Measurement of serum TgAb by ELISA

Thyroid glands were first homogenized and then centrifuged. Mouse Tg (mTg) was collected from the supernatant, as previously described by Imaizumi et al. [26]. Briefly, mouse Tg (mTg) was prepared from frozen mouse thyroids (Pelfreez Biologicals, Rogers, AR). The thyroids were homogenized in PBS and centrifuged at 1000*g* at 4 °C for 10 min, and the supernatant was ultracentrifuged at 425,000*g* for 1 h. The supernatant was then fractionated on a Sephadex G-200 column. The absorbance at 280 nm of the fractions was measured, and the first major peak was pooled and concentrated. Blood was extracted from the hearts of experimental animals and stored at room temperature for at least 2 h, then separated by centrifugation at 314*g* for 20 min and stored at −80 °C. Serum was diluted to 1:100 and evaluated in a 96-well plate that had been pre-incubated with 10 μg/ml of mTg and stored overnight at 4 °C. The plate was washed at least five times and blocked with 1% bovine serum albumin. Peroxidase-labeled goat anti-mouse immunoglobulin G (1:250 dilution, Sigma, USA) and TMB (Sigma, T0440) were used for detection. Absorbance was detected at 450 nm with a microtiter plate reader (Bio-Rad 680, USA).

2.5. Determination of the serum levels of tumor necrosis factor-α (TNF-α), IL-6 and IL-1β

The serum levels of TNF-α, IL-6 and IL-1β were evaluated with ELISA kits (TNF-α, IL-6, IL-1β: R&D Systems) in accordance with the manufacturer's instructions. Absorbance was measured at 450 nm with a microtiter plate reader.

2.6. Flow cytometric analysis of the proportion of Th1/Th2/Th17/Treg cells

Fresh spleen tissues were collected from the three groups of NOD.H-2^{h4} mice and passed through a 200-gauge stainless steel mesh. Mononuclear cells from the spleen were harvested and subsequently stimulated with PMA (Sigma-Aldrich, St. Louis, MO, USA), ionomycin (Sigma-Aldrich, St. Louis, MO, USA) and monensin (BD Biosciences Corp., San Jose, CA, USA) for at least 6 h in a thermostat. For surface staining, cells were stained and permeabilized for intracellular staining. After isolation, lymphocytes were fixed and incubated overnight at 4 °C in the dark. Fixed cells were spun at 500*g* for 10 min and washed twice with 150 μl permeabilization buffer (0.1% saponin and 0.09% sodium azide), then resuspended in 75 μl permeabilization buffer and incubated for 30 min at 4 °C. The cells were stained with anti-CD4-FITC monoclonal antibody (eBioscience, San Diego, CA, USA.), and the intracellular cytokines IL-17 and IFN-γ were detected with monoclonal antibodies against IFN-γ-APC (BD Biosciences Corp., San Jose, CA, USA), IL-4-APC (eBioscience, San Diego, CA, USA), IL-17-APC (eBioscience, San Diego, CA, USA) and FOXP3-APC (eBioscience, San Diego, CA, USA). The rates of apoptosis for T cells were detected by staining with antibodies to CD4, and subsequent Annexin V and PI staining (BD Pharmingen) according to the manufacturer's instructions. Samples were then analyzed with a BD FACS Array (Becton-Dickinson, Fullerton, CA, USA) using Cell quest software.

2.7. Western blot analysis

Thyroid gland samples were quickly frozen in liquid nitrogen and stored at −80 °C. Tissues were homogenized in PBS (pH 7.4) supplemented with 0.05% Triton X-100 and protease inhibitor cocktail (Sigma Aldrich, St. Louis, MO, USA). Proteins were separated with 10% sodium dodecyl sulfate-polyacrylamide gel electrophoresis (Sigma Aldrich, St. Louis, MO, USA) and transferred onto PVDF membranes. After electrophoresis, the gels were equilibrated for 20 min in transfer buffer (25 mM Tris, 190 mM glycine and 20% methanol), and proteins were transferred to PVDF membranes (0.5 h, 30 V), which were then blocked with 5% dried skimmed milk in 100 mM Tris-HCL (pH 7.5) containing 140 mM NaCl and 0.05% Tween 20 for at least 1 h. The membranes were then incubated overnight at 4 °C, with mouse monoclonal anti-caspase 3 antibody and anti-cleaved caspase 3 antibody (1:800, Abcam, Cambridge, United Kingdom), polyclonal rabbit anti-Gas6 antibody (1:1000, R&D Systems), polyclonal rabbit anti-p-MerTK antibody and anti-MerTK antibody (1:1000, R&D Systems), mouse monoclonal anti-NF-κB antibody ([65 kDa subunit] 1:800, Abcam, Cambridge, United Kingdom), mouse monoclonal anti-IκB-α antibody (1:800, Santa Cruz Biotechnologies, Santa Cruz, CA), mouse monoclonal anti-p-Axl antibody and anti-Axl antibody (1:1000, R&D Systems) or polyclonal rabbit anti-β-actin (1:1000, Abcam, Cambridge, United Kingdom) on the same membrane. After being washed three times with blocking solution, the blots were incubated with diluted horseradish peroxidase-conjugated secondary antibodies (1:1000) (Bio-Rad) for 1.0 h at room temperature. The blots were washed extensively and developed with an enhanced chemiluminescence kit (Amersham Pharmacia Biotech, Piscataway, NJ, USA). Western immunoblot bands were quantified with a Bio-Rad calibrated densitometer (GS-800) using the vendor's software (Bio-Rad Laboratories); β-actin was used as an internal reference for analyses.

2.8. Cytoplasmic and nuclear extraction

Extracts of cellular total protein were prepared by physical disruption of cell membranes through repeated freeze-thaw cycles. Briefly, cells were washed with PBS, harvested with trypsin-EDTA and washed twice with PBS to remove traces of trypsin and growth medium. Then cells were resuspended in cytoplasmic buffer (10 mM HEPES, pH 7.9, 10 mM KC1, 0.1 mM EDTA, 0.1 mM EGTA, 1 mM dithiothreitol and protease inhibitors) on ice for 15 min, after which Triton X-100 was added to a final concentration of 0.25%. Intact nuclei were pelleted by centrifugation, and the cytoplasmic extract was immediately frozen. Nuclei were resuspended in high-salt buffer (20 mM HEPES, pH 7.9, 400 mM NaCI, 1 mM EDTA, 1 mM EGTA, 1 mM dithiothreitol and protease inhibitors) for 15 min at 4 °C. The nuclear extract was collected after centrifugation at 13,500*g* for 5 min at 4 °C and immediately frozen.

2.9. Statistical analysis

All statistical analyses were performed using SPSS Software 20.0 (SPSS, Inc., Chicago, IL, USA). Results are shown as means ± standard deviation. One-way analysis of variance (ANOVA) was used to compare the effects of Gas6 treatment in all three groups, and the Bonferroni test was used for pairwise comparisons. GraphPad Prism 5 software was used to analyze data and create graphs. p values < 0.05 were considered statistically significant.

3. Results

3.1. Iodine supplementation reduced GAS6 mRNA and protein levels

We examined the mRNA and protein expression of Gas6 in the thyroid tissue of mice in the NaI and control groups. As shown in Fig. 1A, Gas6 mRNA was significantly lower in the NaI group compared to the control group. Similarly, the protein levels of Gas6 were significantly down-regulated in the NaI group ($p < 0.05$; Fig. 1B and C).

3.2. The effect of Gas6 on serum TgAb titers in NOD.H-2^{h4} mice

As shown in Fig. 2A, the serum levels of TgAb were significantly higher in the NaI group compared to the control group (0.76 ± 0.12 *vs.*

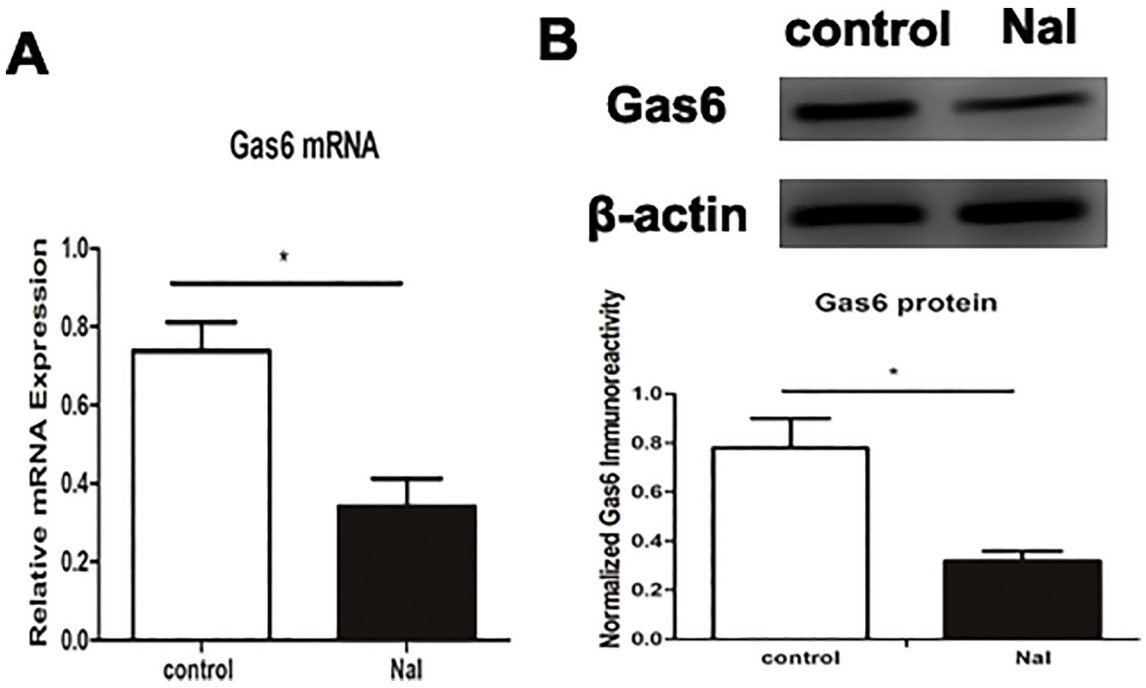

Fig. 1. The mRNA and protein expression of Gas6 in thyroid glands in NaI-treated NOD.H-2^{h4} mice and controls at different time points. A: Real-time PCR analysis of the Gas6 levels in each group. B: Western blot analysis of the Gas6 levels in different groups. The ratio of Gas6/β-actin was determined as the mean net density. NaI group: NOD.H-2^{h4} mice were given 0.005% sodium iodide water; control group: NOD.H-2^{h4} mice were given regular water. Gas6: Growth arrest-specific protein 6. Data are presented as the means ± standard error (n = 8 per group). Statistical analysis was conducted using the *t*-test. *$p < 0.05$ *vs.* control at the same time point.

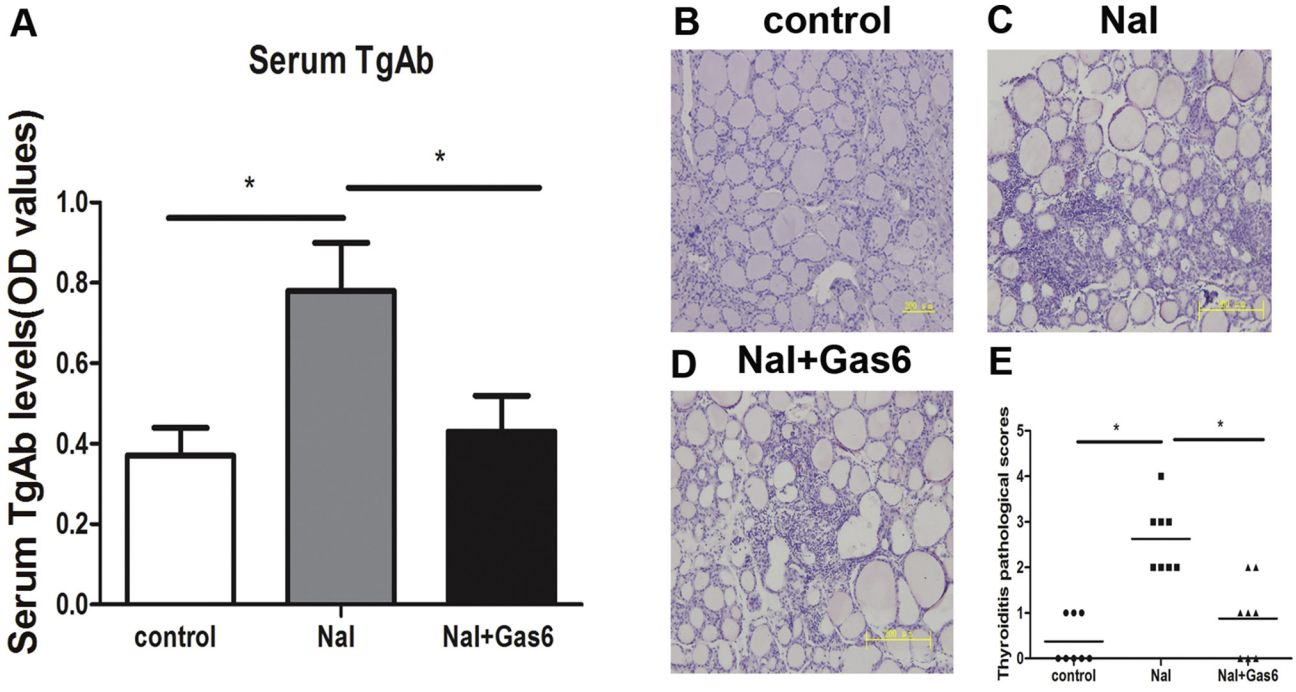

Fig. 2. Serum TgAb levels and thyroid histology of NOD.H-2^{h4} mice.
A: Serum TgAb levels in different groups of NOD.H-2^{h4} mice. B: Control group, 0 severity score. C: NaI group, 3+ severity score D: NaI group with Gas6 supplementation, 1+ severity score. E: Histology scores of thyroid tissue were significantly elevated in the NaI group and decreased significantly after Gas6 administration. Numbers 0–5 represent the thyroiditis scores. Representative histological section of HE-stained thyroid tissues from different groups of NOD.H-2^{h4} mice (HE staining, magnification ×200). NaI group: NOD.H-2^{h4} mice were given 0.005% sodium iodide water; control group: NOD.H-2^{h4} mice were given regular water; Data are presented as the means ± standard error (n = 8 per group). TgAb for control: 0.37 ± 0.07; for NaI: 0.62 ± 0.18; for NaI + Gas6: 0.43 ± 0.09. Gas6: Growth arrest-specific protein 6. One-way ANOVA was used to compare the differences among multiple groups. *$p < 0.05$ *vs.* control at the same time point.

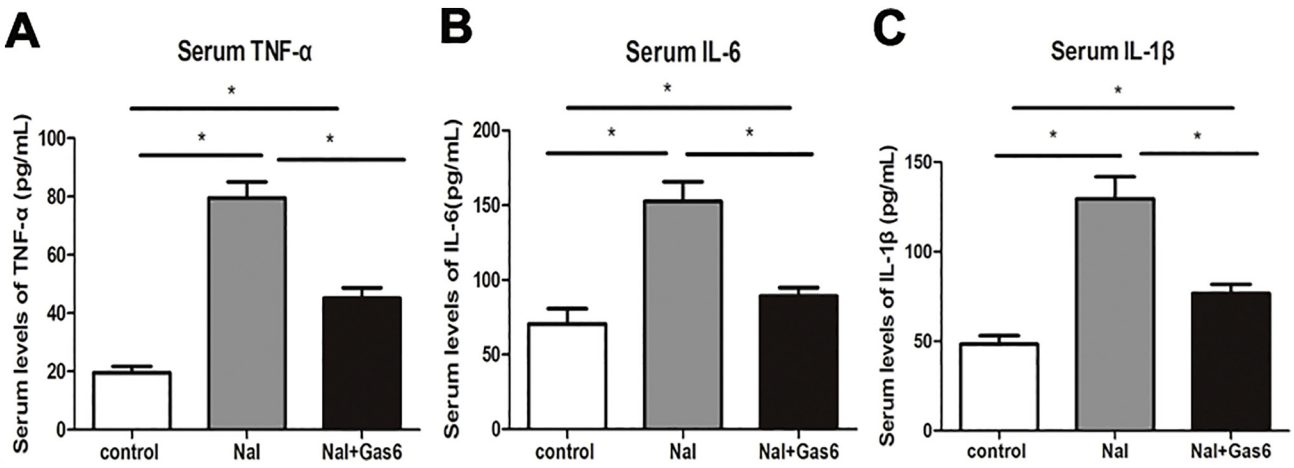

Fig. 3. Serum levels of TNF-α, IL-6 and IL-1β in different groups of NOD.H-2^{h4} mice. NaI group: NOD.H-2^{h4} mice were given 0.005% sodium iodide water; control group: NOD.H-2^{h4} mice were given regular water; Gas6: Growth arrest-specific protein 6. A: Serum TNF-α levels in different groups of NOD.H-2^{h4} mice (pg/ml). B: Serum IL-6 levels in different groups of NOD.H-2^{h4} mice (pg/ml). C: Serum IL-1β levels in different groups of NOD.H-2^{h4} mice (pg/ml). Data are presented as the means ± standard error (n = 8 per group). TNF-α (pg/ml) for control: 19.5 ± 6.23; for NaI: 79.5 ± 15.68; for NaI + Gas6: 45.13 ± 10.22. IL-6 (pg/ml) for control: 70.5 ± 28.77; for NaI: 152.5 ± 37.25; for NaI + Gas6: 89.32 ± 16.53. IL-1β (pg/ml) for control: 48.38 ± 13.46; for NaI: 129.5 ± 34.93; for NaI + Gas6: 76.63 ± 14.74. One-way ANOVA was used to compare the differences among multiple groups. *$p < 0.05$ *vs.* control at the same time point.

0.37 ± 0.07, $p < 0.05$). TgAb titers significantly decreased after rmGas6 treatment (0.43 ± 0.09, $p < 0.05$); TgAb levels were not significantly different between the NaI + Gas6 group and controls.

3.3. The effect of Gas6 on thyroid tissue damage and inflammation in NOD.H-2^{h4} mice

As shown in Fig. 2B and C, after NaI supplementation for 8 weeks, lymphocyte infiltration was observed in the thyroids, and the histological scores ranged from 1+ to 3+. However, these histological changes were markedly improved in the NaI + Gas6 group compared with the NaI group (Fig. 2D). These results were also confirmed by the scores: the NaI + Gas6 group had significantly lower scores than the NaI group ($p < 0.05$; Fig. 2E).

3.4. The effect of Gas6 on serum pro-inflammatory cytokines in NOD.H-2^{h4} mice

The serum levels of IL-1β, IL-6 and TNF-α were significantly higher in the NaI group compared to the controls ($p < 0.05$; Fig. 3A, B and C). However, the concentrations of all three cytokines decreased markedly after rmGas6 treatment ($p < 0.05$; Fig. 3A, B and C). These results suggest that rmGas6 treatment might play an essential role in inhibiting the release of pro-inflammatory cytokines during the development of AIT.

3.5. The effect of Gas6 on the proportions of Th1/Th2/Th17/Treg splenocyte cells in NOD.H-2^{h4} mice

The proportions of $CD4^+$ IFN-γ^+ (Th1), $CD4^+$ IL-4^+ (Th2), $CD4^+$ IL-17^+ (Th17) and $CD4^+$ $FOXP3^+$ (Treg) cells were measured in the splenocytes of NOD.H-2^{h4} mice. As depicted in Fig. 4A, the proportion of Th1 cells was significantly higher in the NaI group compared to the controls (3.42 ± 0.35 *vs.* 6.58 ± 1.21; $p < 0.05$). In addition, the percentages of Th1 cells were dramatically lower in the NaI + Gas6 group compared to the NaI group (3.65 ± 0.41 *vs.* 6.58 ± 1.21; $p < 0.05$). We also found the proportion of Th2 cells significantly increased after iodine treatment (4.82 ± 0.45 *vs.* 11.36 ± 2.03; $p < 0.05$), whereas the proportion of $CD4^+$IL-4^+ cells dramatically decreased after rmGas6 treatment (11.36 ± 2.03 *vs.* 5.07 ± 0.63; $p < 0.05$; Fig. 4B). In addition, the proportion of Th17 cells significantly increased after iodine supplementation (4.03 ± 0.52 *vs.* 7.45 ± 1.36; $p < 0.05$). The proportion of $CD4^+$IL-17^+ cells was significantly lower in the NaI + Gas6 group compared to the NaI group (4.52 ± 0.55 *vs.* 7.45 ± 1.36; $p < 0.05$; Fig. 4C). Moreover, the proportion of $CD4^+$$FOXP3^+$ cells was significantly lower in the NaI group compared to the controls (3.63 ± 0.54 *vs.* 6.04 ± 1.12; $p < 0.05$), whereas the proportion of Treg cells was significantly higher in the NaI + Gas6 group compared to the NaI group (5.89 ± 0.51 *vs.* 3.63 ± 0.54; $p < 0.05$; Fig. 4D).

3.6. The effect of rmGas6 on apoptosis in the thyrocytes and splenocytes of NOD.H-2^{h4} mice

We conducted Western blotting to examine the apoptosis-related protein caspase 3. Caspase 3 expression did not significantly differ among the three groups ($p > 0.05$; Fig. 5A and C), but the protein levels of cleaved caspase 3 were significantly higher in the NaI group ($p < 0.05$; Fig. 5A and B). Cleaved caspase 3 expression significantly decreased after rmGas6 treatment ($p < 0.05$; Fig. 5A and B). No differences were found in the expression of cleaved caspase 3 between the NaI + Gas6 and control groups. In addition, as shown in Fig. 5D, the apoptosis rate in spleen cells was significantly higher in the NaI group compared to the controls (7.44 ± 1.22 *vs.* 19.11 ± 3.52; $p < 0.05$), and was significantly lower in the NaI + Gas6 group compared to the NaI group (11.20 ± 2.35 *vs.* 19.11 ± 3.52; $p < 0.05$).

3.7. The effect of Gas6 on TAM receptor expression in the thyroid gland in NOD.H-2^{h4} mice

Gas6 protein levels were significantly lower in the thyroids of animals exposed to iodine ($p < 0.05$; Fig. 6A and B); these results were consistent with the mRNA expression results. In addition, Gas6 treatment augmented the expression of Gas6 protein ($p < 0.05$; Fig. 6A and B). Axl and MerTK are TAM receptors, and are phosphorylated after binding Gas6. Although no changes in Axl activation were detected in the NaI group compared to the control group ($p > 0.05$; Fig. 6A and C), levels of phosphorylated MerTK increased after iodine supplementation ($p < 0.05$); this change was more enhanced in the NaI + Gas6 group than in the NaI group ($p < 0.05$; Fig. 6A and D).

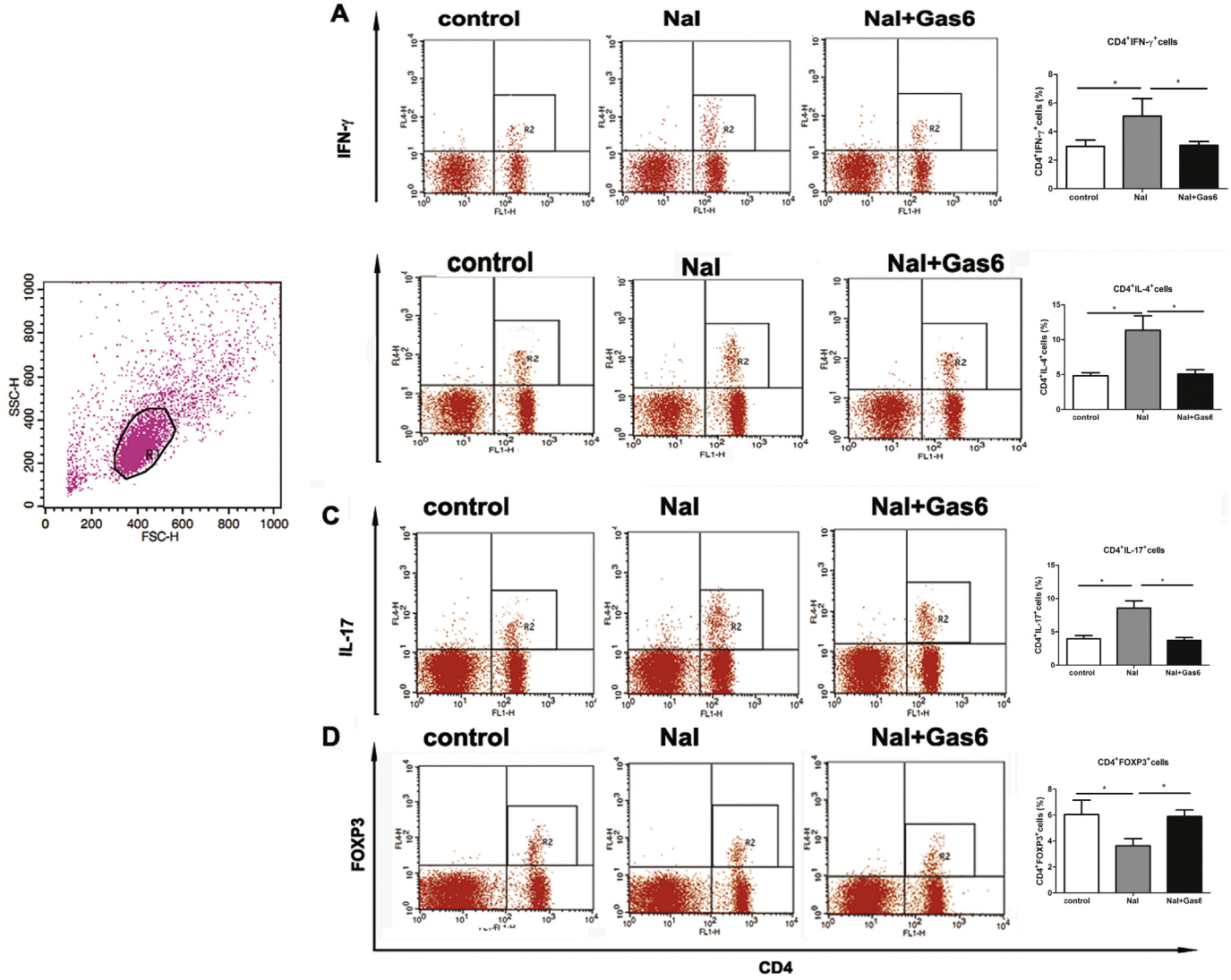

Fig. 4. The percentage of Th1/Th2/Th17/Treg cells in spleen cells in different groups of NOD.H-2^{h4} mice. A: Flow cytometry dot plots from the three groups depicting IFN-γ expression in CD4 enriched monocytes (left panels). The numbers in the right quadrants represent the percentages of $CD4^+IFN\text{-}\gamma^+$ cells in each group. B: Flow cytometry dot plots from the three groups, depicting IL-4 expression in CD4 enriched monocytes (left panels). The numbers in the right quadrants represent the percentage of $CD4^+IL\text{-}4^+$ cells in each group. C: Flow cytometry dot plots from each group depicting IL-17 expression in CD4-enriched monocytes (left panels). Percentages of $CD4^+IL\text{-}17^+$ cells were compared among the three groups (middle panels). D: Flow cytometry dot plots from the three groups, depicting FOXP3 expression in CD4-enriched monocytes (right panels). Data are presented as the means ± standard error (n = 8 per group). $CD4^+$ $IFN\text{-}\gamma^+$ cell percentage for control: 3.42 ± 0.35; for NaI: 6.58 ± 1.21; for NaI + Gas6: 3.65 ± 0.41. $CD4^+$ $IL\text{-}4^+$ percentage for control: 4.82 ± 0.45; for NaI: 11.36 ± 2.03; for NaI + Gas6: 3.65 ± 0.41. $CD4^+IL\text{-}17^+$ cell percentage for control: 4.03 ± 0.52; for NaI: 7.45 ± 1.36; for NaI + Gas6: 4.52 ± 0.55. $CD4^+FOXP3^+$ cell percentage for control: 3.63 ± 0.54; for NaI: 6.04 ± 1.12; for NaI + Gas6: 3.89 ± 0.51. One-way ANOVA was used to compare the differences among multiple groups. *$p < 0.05$ *vs.* control at the same time point. NaI group: NOD.H-2^{h4} mice were given 0.005% sodium iodide water; control group: NOD.H-2^{h4} mice were given regular water; Gas6: Growth arrest-specific protein 6.

3.8. The effect of Gas6 on the activation of NF-κB in the thyroid gland in NOD.H-2^{h4} mice

To investigate NF-κB activation in the Gas6-dependent pathway during AIT, we measured the levels of IκB-α protein, an endogenous antagonist of NF-κB, by Western blotting. As shown in Fig. 7A and C, the levels of IκB-α in the thyroid were lower in the NaI group than in the control group ($p < 0.05$); these changes, however, were inhibited by rmGas6 supplementation ($p < 0.05$). To further verify whether the decrease in IκB-α level was correlated with increased nuclear translocation of NF-κB, we examined the protein expression of NF-κB in thyroid tissues by Western blotting. As shown in Fig. 7A and B, a significantly higher expression of total NF-κB was detected in the NaI group compared to the control group ($p < 0.05$). However, these marked changes were decreased by Gas6 treatment ($p < 0.05$). Moreover, no differences in the NF-κB cytoplasmic fraction were found after treatment with rmGas6 ($p > 0.05$ Fig. 7D and E), but a marked decrease in the NF-κB nuclear fraction was detected after rmGas6 supplementation ($p < 0.05$ Fig. 7D and F).

4. Discussion

In this work, we found that Gas6 mRNA and protein expression were significantly diminished in the thyroid in iodine-induced NOD.H-2^{h4} mice. This study also revealed that rmGas6 treatment significantly decreased the level of lymphocyte infiltration in the thyroid; decreased the levels of pro-inflammatory cytokines and cleaved caspase 3, as well as the apoptosis rate; and regulated TAM receptors and downstream mediators. These results indicated that Gas6 may be involved in the development of autoimmune thyroiditis and may play a crucial role in

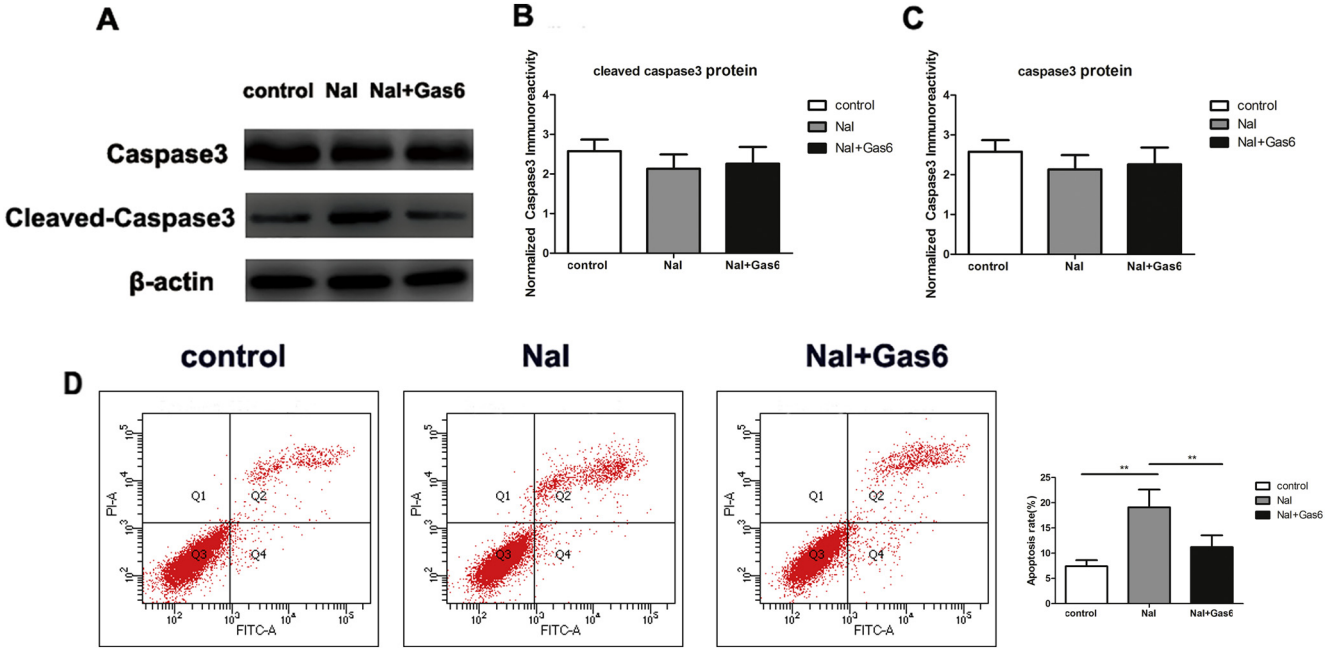

Fig. 5. The effect of rmGas6 on apoptosis in the thyrocytes and splenocytes in NOD.H-2^{h4} mice. A: Western blot analysis of caspase3 levels in different groups. B: The cleaved caspase3/β-actin ratio was determined as the mean net density. C: The total caspase3/β-actin ratio was determined as the mean net density D: Flow cytometry dot plots from the three groups, depicting apoptotic cells in the spleen in CD4-enriched monocytes. Data are presented as the means ± standard error (n = 8 per group). One-way ANOVA was used to compare the differences among multiple groups. *$p < 0.05$ *vs.* control at the same time point. NaI group: NOD.H-2^{h4} mice were given 0.005% sodium iodide water; control group: NOD.H-2^{h4} mice were given regular water; Gas6: Growth arrest-specific protein 6.

protecting against thyroid injury.

The loss of immune tolerance to self-antigens in the thyroid is the mechanism underlying AIT. Genetic background, immunological regulation, and environmental factors may also contribute to the development of AIT. Iodine is a major environmental cause of AIT. Previous studies have demonstrated that excessive levels of iodine induce AIT and increase the severity of lymphocyte infiltration in NOD.H-2^{h4} mice, as reported in a mouse model of AIT and in humans [1,3,27,28]. The sequence of events occurring between the appearance of thyrocyte apoptosis and the onset of thyroiditis in excess iodine-induced AIT must be elucidated. We suggest that apoptosis, which appears earlier than inflammatory infiltration, may be the initial event in AIT in NOD.H-2^{h4} mice. He et al. consistently observed high levels of apoptosis in the thyroid glands, even as early as 2 weeks in an HI group of NOD.H-2^{h4} mice before cellular infiltration, which was first detected at 4 weeks [29].

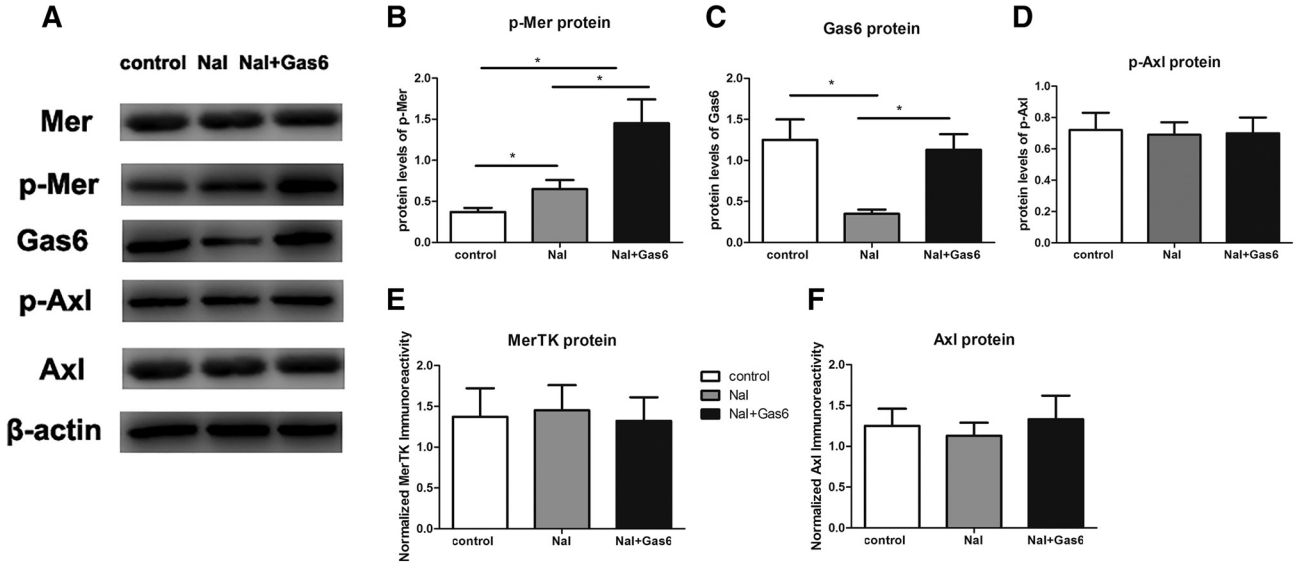

Fig. 6. Protein expression of TAM receptors in the thyroid glands in NOD.H-2^{h4} mice. A: Western blot analysis of Gas6 and phosphorylation of Axl and Mer in each group. B: The ratio of phosphorylated-Mer/β-actin was determined as the mean net density. C: The ratio of Gas6/β-actin was determined as the mean net density. D: The ratio of phosphorylation-Axl/β-actin was determined as the mean net density. E: The ratio of Mer/β-actin was determined as the mean net density. F: The ratio of Axl/β-actin was determined as the mean net density. Data are presented as the means ± standard error (n = 8 per group). One-way ANOVA was used to compare the differences among multiple groups. *$p < 0.05$ *vs.* control at the same time point. NaI group: NOD.H-2^{h4} mice were given 0.005% sodium iodide water; control group: NOD.H-2^{h4} mice were given regular water; Gas6: Growth arrest-specific protein 6.

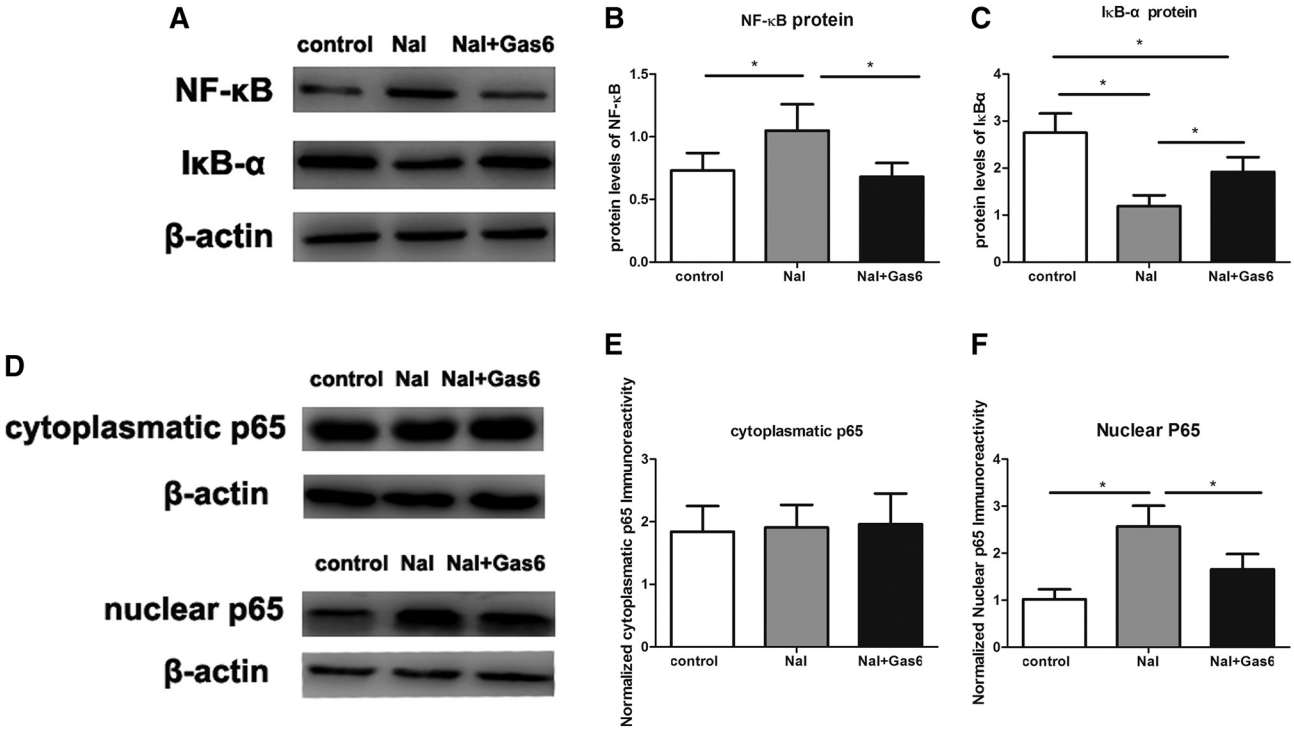

Fig. 7. Protein expression of NF-κB and IκB-α in the thyroid glands in NOD.H-2^{h4} mice. A: Western blot analysis of NF-κB and IκB-α in each group. B: The ratio of NF-κB/β-actin was determined as the mean net density. C: The ratio of IκB-α/β-actin was determined as the mean net density. D: Western blot analysis of cytoplasmic and nuclear NF-κB in each group. E: The ratio of cytoplasmic NF-κB/β-actin was determined as the mean net density. F: The ratio of nuclear NF-κB/β-actin was determined as the mean net density. Data are presented as the means ± standard error (n = 8 per group). One-way ANOVA was used to compare the differences among multiple groups. *$p < 0.05$ *vs.* control at the same time point. NaI group: NOD.H-2^{h4} mice were given 0.005% sodium iodide water; control group: NOD.H-2^{h4} mice were given regular water; Gas6: Growth arrest-specific protein 6.

We found that the mRNA and protein levels of Gas6 were reduced in the AIT mouse model. Gas6 was identified as a link between the phagocytes and the molecular target *via* the enhanced clearance of apoptotic cells. Gas6 plays an important role in the regulation of inflammatory diseases. Moreover, plasma levels of Gas6 are inversely associated with the levels of pro-inflammatory cytokines in patients with diabetes [30]. Excessive iodine intake is known to contribute to apoptosis in the thyroid [31]. The reduced levels of Gas6 mRNA and protein expression in iodine-treated NOD.H-2^{h4} mice may be due to the excessive production of unclear apoptotic cells and the inflammatory response.

In this study, mice in the NaI group showed lymphocyte infiltration into the thyroid, severe thyroiditis pathological scores and higher serum TgAb titers than those in the control group. However, severity scores, lymphocytic infiltration into thyroid tissue and serum levels of TgAb were decreased in those mice treated with rmGas6 *via* intravenous injection. TAM signaling has been demonstrated to contribute to the pathogenesis of autoimmune diseases and the removal of apoptotic cells and is therefore associated with the abnormal production of pro-inflammatory cytokines by immune cells [32]. Gas6 and its receptors are regulators of the innate immune system, inhibiting the anti-inflammatory response by repressing the production of pro-inflammatory cytokines *via* immune cells such as dendritic cells and macrophages [33]. *In vitro* studies have found that TLR activation up-regulates TAMs *via* the type I interferon pathway, thus resulting in up-regulation of suppressor of cytokine signaling proteins 1 and 3, which in turn activate the inflammatory response through activation of antigen-presenting cells [14]. This finding suggests that TAM/Gas6 signaling plays an essential role in the anti-inflammatory response [9].

It has been previously reported that rmGas6 decreased mortality in mice, as well as the production of cytokines and the extent of lymphocyte infiltration in a mouse model of sepsis [34]. After the intracerebral administration of Gas6, experimental autoimmune encephalomyelitis mice showed lower levels of demyelination and higher remyelination than controls. Moreover, higher clinical scores and delayed recovery from tissue impairment were observed after induction of experimental autoimmune encephalomyelitis in Gas6 knockout mice. Furthermore, inflammation is more predominant in the medulla spinalis, the production of proinflammatory cytokines is elevated, and infiltration of macrophages is severer [35]. These results are consistent with our current results, thus suggesting that the anti-inflammatory effect of rmGas6 is likely to play an important role in decreasing tissue damage by inhibiting the inflammatory response.

We also observed a significant decrease in the serum levels of TNF-α, IL-6 and IL-1β in NOD.H-2^{h4} mice after rmGas6 treatment. Higher concentrations of these pro-inflammatory cytokines have been identified to regulate organ damage in AIT mouse model [28]. This result suggests that Gas6 administration is likely to decrease tissue damage by attenuating the inflammatory response.

The expression of T cell subsets in splenocytes was also measured in AIT mouse model. $CD4^+$ T cells consist of Th1/Th2/Th17/Treg subsets. The Th1-mediated response plays a critical role in the development of AIT [36]. The Th17 subset has also been suggested to be associated with thyroid autoimmunity [37]. Our study showed that the proportions of $CD4^+$ IFN-γ^+ (Th1 representative cytokine), $CD4^+$IL-4^+ (Th2 representative cytokine) and $CD4^+$IL-17^+ (Th17 representative cytokine) were significantly higher in mice receiving iodine supplementation than in controls, and the up-regulation of Th1, Th2 and Th17 subsets in spleen cells was significantly lower in the NaI group compared to the rmGas6 group, whereas the number of $CD4^+$ $FOXP3^+$ cells was significantly lower in the NaI group and higher after rmGas6 treatment. These results suggest that the protective effect of Gas6 may play an important role in inflammation through regulation of the distribution of the T cell subset.

In the present study, we also discovered a marked decrease in the protein levels of cleaved caspase 3 in the thyroid gland and the apoptosis rate in spleen cells after inducing AIT with rmGas6 supplementation. Caspase 3 belongs to a sub-family of endoproteases that play a major role in homeostasis by regulating the immune response and cell apoptosis [38]. Gas6 stimulates the ingestion of apoptotic debris by macrophages to clear necrotic cells [39]. Moreover, a deficiency in the ability to clear apoptotic cells may cause secondary necrosis, thus resulting in the production of pro-inflammatory cytokines and tissue damage [40]. Elevated numbers of apoptotic thyrocytes and defective removal of apoptotic cells by macrophages have been observed in NOD.H-2^{h4} mice [41]. The activation of immune cells may play an important role in triggering thyrocyte destruction during the inflammatory response; furthermore the microenvironment of the thyroid may be responsible for promoting apoptosis [42–44]. Therefore, the upregulation of phagocytosis may be a potent mechanism through which rmGas6 administration decreases thyroid damage in AIT.

Axl and MerTK are TAM receptors that are phosphorylated after binding Gas6. In this study, no changes in Axl activation were found across the three groups. However, the levels of p-MerTK were increased after iodine supplementation; this increase was more enhanced in the rmGas6 treatment group compared to the NaI group. Llacuna et al. have previously demonstrated that MerTK is phosphorylated in mice subjected to ischemia/reperfusion, and this response is inhibited in Gas6 knockout mice [34]. Interestingly, Gas6 inhibits the secretion of IL-1β and TNF-α in response to lipopolysaccharide by MerTK activation [18]. Furthermore, the binding affinity of Gas6 for MerTK, but not Tyro3 or Axl, leads to MerTK phosphorylation, which prevents the activation of NF-κB signaling. Weinger and colleagues have further reported that Gas6 is restrained by the extracellular portion of MerTK, which inactivates the biological effects of Gas6 [45]. A previous study has also found that Gas6 function is restricted by the soluble form of MerTK, through inhibition of the phagocytosis of apoptotic cells by macrophages [46]. Our results, and those of previous studies, elucidate the effect of Gas6-MerTK binding, which induces an anti-inflammatory response against thyroid injury in AIT.

To further evaluate the potential mechanism underlying the anti-inflammatory effect of Gas6, we examined NF-κB and its inhibitor in the thyroid gland. We found that NF-κB protein was significantly up-regulated in the thyroids of mice in the NaI group compared with the control group, whereas Gas6 treatment markedly inhibited this upregulation. Indeed, in NOD.H-2^{h4} mice, no differences in activated NF-κB in the cytoplasmic fraction or increases in the nuclear fraction were observed. Moreover, we examined changes in the expression of IκB-α, which inhibits NF-κB by altering binding affinity, thereby preventing NF-κB translocation. In this study, the diminished protein expression of IκB-α in the thyroid gland was elevated by rmGas6 treatment, thus suggesting that rmGas6 blocks the phosphorylation of IκB-α, thereby attenuating the decrease in IκB-α and maintaining NF-κB in an inert status. In addition, we previously reported that the active form of NF-κB is elevated in thyroid tissues after iodine treatment in NOD.H-2^{h4} mice, and the persistent secretion of pro-inflammatory cytokines mediated by NF-κB plays an essential part in iodine-induced AIT [28]. IκB-α plays a crucial role in the nuclear translocation of NF-κB. Our present results suggest that rmGas6 supplementation prevents the translocation of NF-κB to the nucleus *via* regulation of the Gas6/TAM pathway.

5. Conclusion

Gas6 is a multifunctional protein that assists in the regulation of phagocytosis and inflammation. In an iodine-induced autoimmune thyroiditis model, tissue destruction, the inflammatory response, and apoptosis in the thyroid were significantly decreased after treatment with rmGas6. Our results show that rmGas6 exerts an anti-inflammatory effect in a mouse model of AIT. Thus, rmGas6 may have therapeutic potential for the treatment of patients with autoimmune thyroiditis.

Conflicts of interest

The authors declare no conflicts of interest.

Acknowledgments

This study was supported by the National Natural Science Foundation of China (grants 81400777, 81570708, 81870539, 81700688, 81870538), the Doctoral Start-up Foundation of Liaoning Province (grant 201501012, 201601132), the Excellent Youth Scientific program in China Medical University (grant YQ20170007) and the Program for Liaoning Excellent Talents in University (grant LJQ2015115).

References

[1] C.L. Burek, M.V. Talor, Environmental triggers of autoimmune thyroiditis, J. Autoimmun. 33 (3–4) (2009) 183–189.
[2] A.P. Weetman, Hypothyroidism: screening and subclinical disease, BMJ 314 (7088) (1997) 1175–1178.
[3] H. Braley-Mullen, G.C. Sharp, B. Medling, H. Tang, Spontaneous autoimmune thyroiditis in NOD.H-2h4 mice, J. Autoimmun. 12 (3) (1999) 157–165.
[4] C. Scaffidi, S. Kirchhoff, P.H. Krammer, M.E. Peter, Apoptosis signaling in lymphocytes, Curr. Opin. Immunol. 11 (3) (1999) 277–285.
[5] D.L. Vaux, S.J. Korsmeyer, Cell death in development, Cell 96 (2) (1999) 245–254.
[6] J.D. Bretz, E. Mezosi, T.J. Giordano, P.G. Gauger, N.W. Thompson, J.R. Baker, Jr, Inflammatory cytokine regulation of TRAIL-mediated apoptosis in thyroid epithelial cells, Cell Death Differ. 9 (3) (2002) 274–286.
[7] H.M. Seitz, T.D. Camenisch, G. Lemke, H.S. Earp, G.K. Matsushima, Macrophages and dendritic cells use different Axl/Mertk/Tyro3 receptors in clearance of apoptotic cells, J. Immunol. 178 (9) (2007) 5635–5642.
[8] P.L. Cohen, R. Caricchio, V. Abraham, T.D. Camenisch, J.C. Jennette, R.A. Roubey, H.S. Earp, G. Matsushima, E.A. Reap, Delayed apoptotic cell clearance and lupus-like autoimmunity in mice lacking the c-mer membrane tyrosine kinase, J. Exp. Med. 196 (1) (2002) 135–140.
[9] C.V. Rothlin, E.A. Carrera-Silva, L. Bosurgi, S. Ghosh, TAM receptor signaling in immune homeostasis, Annu. Rev. Immunol. 33 (2015) 355–391.
[10] K. Nagata, K. Ohashi, T. Nakano, H. Arita, C. Zong, H. Hanafusa, K. Mizuno, Identification of the product of growth arrest-specific gene 6 as a common ligand for Axl, Sky, and Mer receptor tyrosine kinases, J. Biol. Chem. 271 (47) (1996) 30022–30027.
[11] T.N. Stitt, G. Conn, M. Gore, C. Lai, J. Bruno, C. Radziejewski, K. Mattsson, J. Fisher, D.R. Gies, P.F. Jones, et al., The anticoagulation factor protein S and its relative, Gas6, are ligands for the Tyro 3/Axl family of receptor tyrosine kinases, Cell 80 (4) (1995) 661–670.
[12] D. Prasad, C.V. Rothlin, P. Burrola, T. Burstyn-Cohen, Q. Lu, P. Garcia de Frutos, G. Lemke, TAM receptor function in the retinal pigment epithelium, Mol. Cell. Neurosci. 33 (1) (2006) 96–108.
[13] G. Lemke, C.V. Rothlin, Immunobiology of the TAM receptors, Nat. Rev. Immunol. 8 (5) (2008) 327–336.
[14] C.V. Rothlin, S. Ghosh, E.I. Zuniga, M.B. Oldstone, G. Lemke, TAM receptors are pleiotropic inhibitors of the innate immune response, Cell 131 (6) (2007) 1124–1136.
[15] W.H. Shao, Y. Zhen, R.A. Eisenberg, P.L. Cohen, The Mer receptor tyrosine kinase is expressed on discrete macrophage subpopulations and mainly uses Gas6 as its ligand for uptake of apoptotic cells, Clin. Immunol. 133 (1) (2009) 138–144.
[16] L. Bellido-Martin, P.G. de Frutos, Vitamin K-dependent actions of Gas6, Vitam. Horm. 78 (2008) 185–209.
[17] I. Hasanbasic, J. Cuerquis, B. Varnum, M.D. Blostein, Intracellular signaling pathways involved in Gas6-Axl-mediated survival of endothelial cells, Am. J. Physiol. Heart Circ. Physiol. 287 (3) (2004) H1207–H1213.
[18] F. Alciato, P.P. Sainaghi, D. Sola, L. Castello, G.C. Avanzi, TNF-alpha, IL-6, and IL-1 expression is inhibited by GAS6 in monocytes/macrophages, J. Leukoc. Biol. 87 (5) (2010) 869–875.
[19] T. Deng, Y. Zhang, Q. Chen, K. Yan, D. Han, Toll-like receptor-mediated inhibition of Gas6 and ProS expression facilitates inflammatory cytokine production in mouse macrophages, Immunology 135 (1) (2012) 40–50.
[20] Y.J. Lee, J.Y. Han, J. Byun, H.J. Park, E.M. Park, Y.H. Chong, M.S. Cho, J.L. Kang, Inhibiting Mer receptor tyrosine kinase suppresses STAT1, SOCS1/3, and NF-kappaB activation and enhances inflammatory responses in lipopolysaccharide-induced acute lung injury, J. Leukoc. Biol. 91 (6) (2012) 921–932.
[21] C. Ekman, A. Linder, P. Akesson, B. Dahlback, Plasma concentrations of Gas6 (growth arrest specific protein 6) and its soluble tyrosine kinase receptor sAxl in sepsis and systemic inflammatory response syndromes, Crit. Care 14 (4) (2010) R158.
[22] L. Llacuna, C. Barcena, L. Bellido-Martin, L. Fernandez, M. Stefanovic, M. Mari, C. Garcia-Ruiz, J.C. Fernandez-Checa, P. Garcia de Frutos, A. Morales, Growth arrest-specific protein 6 is hepatoprotective against murine ischemia/reperfusion

injury, Hepatology 52 (4) (2010) 1371–1379.
[23] K.J. Png, N. Halberg, M. Yoshida, S.F. Tavazoie, A microRNA regulon that mediates endothelial recruitment and metastasis by cancer cells, Nature 481 (7380) (2011) 190–194.
[24] T. Shibata, U.B. Ismailoglu, N.A. Kittan, A.P. Moreira, A.L. Coelho, G.L. Chupp, S.L. Kunkel, N.W. Lukacs, C.M. Hogaboam, Role of growth arrest-specific gene 6 in the development of fungal allergic airway disease in mice, Am. J. Respir. Cell Mol. Biol. 51 (5) (2014) 615–625.
[25] E.M. Allen, M.C. Appel, L.E. Braverman, The effect of iodide ingestion on the development of spontaneous lymphocytic thyroiditis in the diabetes-prone BB/W rat, Endocrinology 118 (5) (1986) 1977–1981.
[26] M. Imaizumi, A. Pritsker, M. Kita, L. Ahmad, P. Unger, T. Davies, Pregnancy and murine thyroiditis: thyroglobulin immunization leads to fetal loss in specific allogeneic pregnancies, Endocrinology 142 (2) (2001) 823–829.
[27] L. Rasooly, C.L. Burek, N.R. Rose, Iodine-induced autoimmune thyroiditis in NOD-H-2h4 mice, Clin. Immunol. Immunopathol. 81 (3) (1996) 287–292.
[28] C. Li, S. Peng, X. Liu, C. Han, X. Wang, T. Jin, S. Liu, W. Wang, X. Xie, X. He, H. Zhang, L. Shan, C. Fan, Z. Shan, W. Teng, Glycyrrhizin, a direct HMGB1 antagonist, ameliorates inflammatory infiltration in a model of autoimmune thyroiditis via inhibition of TLR2-HMGB1 signaling, Thyroid Off. J. Am. Thyroid Assoc. 27 (5) (2017) 722–731.
[29] X. He, C. Xiong, A. Liu, W.P. Teng, Phagocytosis deficiency of macrophages in NOD.H-2_{h4} mice accelerates the severity of iodine-induced autoimmune thyroiditis, Biol. Trace Elem. Res. 184 (1) (2018) 196–205.
[30] Y.J. Hung, C.H. Lee, N.F. Chu, Y.S. Shieh, Plasma protein growth arrest-specific 6 levels are associated with altered glucose tolerance, inflammation, and endothelial dysfunction, Diabetes Care 33 (8) (2010) 1840–1844.
[31] S. Fountoulakis, G. Philippou, A. Tsatsoulis, The role of iodine in the evolution of thyroid disease in Greece: from endemic goiter to thyroid autoimmunity, Hormones (Athens) 6 (1) (2007) 25–35.
[32] Q. Lu, G. Lemke, Homeostatic regulation of the immune system by receptor tyrosine kinases of the Tyro 3 family, Science 293 (5528) (2001) 306–311.
[33] X. Feng, T. Deng, Y. Zhang, S. Su, C. Wei, D. Han, Lipopolysaccharide inhibits macrophage phagocytosis of apoptotic neutrophils by regulating the production of tumour necrosis factor alpha and growth arrest-specific gene 6, Immunology 132 (2) (2011) 287–295.
[34] M.D. Giangola, W.L. Yang, S.R. Rajayer, J. Nicastro, G.F. Coppa, P. Wang, Growth arrest-specific protein 6 attenuates neutrophil migration and acute lung injury in sepsis, Shock 40 (6) (2013) 485–491.
[35] R.C. Gruber, A.K. Ray, C.T. Johndrow, H. Guzik, D. Burek, P.G. de Frutos, B. Shafit-Zagardo, Targeted GAS6 delivery to the CNS protects axons from damage during experimental autoimmune encephalomyelitis, J. Neurosci. 34 (49) (2014) 16320–16335.
[36] S. Yu, G.C. Sharp, H. Braley-Mullen, Dual roles for IFN-gamma, but not for IL-4, in spontaneous autoimmune thyroiditis in NOD.H-2h4 mice, J. Immunol. 169 (7) (2002) 3999–4007.
[37] N. Figueroa-Vega, M. Alfonso-Perez, I. Benedicto, F. Sanchez-Madrid, R. Gonzalez-Amaro, M. Marazuela, Increased circulating pro-inflammatory cytokines and Th17 lymphocytes in Hashimoto's thyroiditis, J. Clin. Endocrinol. Metab. 95 (2) (2010) 953–962.
[38] S.M. Man, T.D. Kanneganti, Converging roles of caspases in inflammasome activation, cell death and innate immunity, Nat. Rev. Immunol. 16 (1) (2016) 7–21.
[39] Y. Ishimoto, K. Ohashi, K. Mizuno, T. Nakano, Promotion of the uptake of PS liposomes and apoptotic cells by a product of growth arrest-specific gene, gas6, J. Biochem. 127 (3) (2000) 411–417.
[40] M.T. Silva, A. do Vale, N.M. dos Santos, Secondary necrosis in multicellular animals: an outcome of apoptosis with pathogenic implications, Apoptosis 13 (4) (2008) 463–482.
[41] P. Kolypetri, G. Carayanniotis, Apoptosis of NOD.H2 h4 thyrocytes by low concentrations of iodide is associated with impaired control of oxidative stress, Thyroid 24 (7) (2014) 1170–1178.
[42] S.H. Wang, J.D. Bretz, E. Phelps, E. Mezosi, P.L. Arscott, S. Utsugi, J.R. Baker, Jr., A unique combination of inflammatory cytokines enhances apoptosis of thyroid follicular cells and transforms nondestructive to destructive thyroiditis in experimental autoimmune thyroiditis, J. Immunol. 168(5) (2002) 2470–4.
[43] S.H. Wang, M. Van Antwerp, R. Kuick, P.G. Gauger, G.M. Doherty, Y.Y. Fan, J.R. Baker, Jr., Microarray analysis of cytokine activation of apoptosis pathways in the thyroid, Endocrinology 148(10) (2007) 4844–52.
[44] E. Mezosi, S.H. Wang, S. Utsugi, L. Bajnok, J.D. Bretz, P.G. Gauger, N.W. Thompson, J.R. Baker, Jr., Induction and regulation of Fas-mediated apoptosis in human thyroid epithelial cells, Mol. Endocrinol. 19(3) (2005) 804–11.
[45] J.G. Weinger, K.M. Omari, K. Marsden, C.S. Raine, B. Shafit-Zagardo, Up-regulation of soluble Axl and Mer receptor tyrosine kinases negatively correlates with Gas6 in established multiple sclerosis lesions, Am. J. Pathol. 175 (1) (2009) 283–293.
[46] S. Sather, K.D. Kenyon, J.B. Lefkowitz, X. Liang, B.C. Varnum, P.M. Henson, D.K. Graham, A soluble form of the Mer receptor tyrosine kinase inhibits macrophage clearance of apoptotic cells and platelet aggregation, Blood 109 (3) (2007) 1026–1033.